

Water film washers and mixers: their rotational modes and electro-hydrodynamical flows induced by square-wave electric fields

Zhong-Qiang Liu · Ying-Jun Li · Kong-Yin Gan ·
Su-Rong Jiang · Guang-Cai Zhang

Received: 24 May 2012 / Accepted: 14 August 2012 / Published online: 16 October 2012
© Springer-Verlag 2012

Abstract Our study indicates suspended water films, driven by crossed square-wave electric fields, may act as “washers”, “centrifuges” and “mixers”. Based on our recent model successfully describing experimentally observed electro-hydrodynamical flows in water films, we derive conditions for generating specific rotational flows. Our main findings, which are advantageous for microfluidic devices and basic research, are as follows: (1) the film’s rotational patterns depend on the phase difference $\Delta\varphi$ and frequencies f of the applied fields. (2) For $\Delta\varphi = \pi/2$ and $f \sim 10^{-1} - 10^0$ Hz, the film exhibits symmetrical reciprocating rotations, i.e. it constitutes a washer. (3) For $\Delta\varphi = 0$ and any f , it exhibits an ordinary anticlockwise (or clockwise) rotation, i.e. it constitutes a centrifuge or motor. (4) For $\Delta\varphi$ with other values and f below 1 Hz, it exhibits asymmetrical reciprocating rotations, it constitutes an asymmetrical mixer.

Keywords Electro-hydrodynamical motions · Suspended water film · Square-wave electric fields · Rotation of liquid film

1 Introduction

Unique properties of flows in liquid films induced by electric fields are of great importance in microfluidic devices (Squires and Quake 2005; El-Ali et al. 2006). Applied electric fields can produce well-controlled electro-hydrodynamic (EHD) flows in freely suspended liquid films (Sonin 1998; Faetti et al. 1983a, b; Morris et al. 1990; Daya et al. 1997; Ramos et al. 1998). Recently, Shirsavar et al. made an important breakthrough: they succeeded to induce EHD flows in suspended polar liquid films, including water at ambient conditions. The flows can be induced by applying crossed direct current (DC) or alternating current (AC) electric fields, i.e., insertion of the film in an external electric field E_{ext} which crosses an electrolysis field E_{el} . The latter induces an electrolysis current density J_{el} ($J_{\text{el}} = \gamma E_{\text{el}}$, γ denotes the conductivity of the liquid) (Shirsavar et al. 2006, 2011; Amjadi et al. 2008, 2009). E_{ext} and E_{el} may induce rotational and vibrational flows. The direction and speed of the rotations can be controlled by manipulating the direction and strength of E_{ext} and E_{el} . These qualities led to the device’s name “liquid film motor”. (In the rest of this paper, we will refer to a rotating polar liquid film driven by DC or AC fields, respectively, as DC motor and AC motor.) The main experimentally observed characteristics of the DC motor are (Amjadi et al. 2009): (a) For non-vanishing E_{ext} and J_{el} , whenever E_{ext} or the electrolysis voltage U_{el} exceeds a threshold, the film rotates. The threshold fields obey a simple scaling relation $E_{\text{ext}} U_{\text{el}} = \text{Const.}$ (b) The rotation

Z.-Q. Liu · Y.-J. Li (✉) · K.-Y. Gan
State Key Laboratory for GeoMechanics and Deep
Underground Engineering, SMCE, China University of Mining
and Technology, Beijing, China
e-mail: lyj@aphy.iphy.ac.cn

Z.-Q. Liu
e-mail: phyzhqliu@yahoo.com.cn

K.-Y. Gan
e-mail: gankongyin@yahoo.com.cn

Z.-Q. Liu · S.-R. Jiang
Department of Physics, Qufu Normal University, Qufu, China

S.-R. Jiang
e-mail: jiangsurong@yahoo.com.cn

G.-C. Zhang
National Key Laboratory of Computational Physics,
Institute of Applied Physics and Computational Mathematics,
Beijing, China
e-mail: zhang_guangcai@iapcm.ac.cn

direction obeys a simple right-hand rule $\mathbf{E}_{\text{ext}} \times \mathbf{J}_{\text{el}}$. (c) Angular velocity measurements show that the region near the center of the film rotates faster than that near the border. As to the AC motor, experiments showed that the fields' frequencies, magnitudes and the difference in their phases strongly influence the dynamics of the liquid film: (a) Whenever, the frequencies of \mathbf{E}_{ext} and \mathbf{U}_{el} are exactly the same, the film may rotate. The phase difference of the fields and their magnitudes affect the threshold for rotation and the angular velocities. The dynamical characteristics of the rotation, measured for frequencies in the range of 50 Hz up to 40 kHz, are the same as those of the DC case. (b) Fields with different frequencies induce vibrations with beating frequencies. Such fields do not lead to any rotation.

Notwithstanding experimentally deduced insights that it is the intrinsic polarity of the liquid that is responsible for generating the rotational EHD flows, while the edge effects do not play a significant role, theoreticians attempted to develop a model based on the edge effects (Shirsavar et al. 2009). Their model provides a possible explanation for the rotation of the DC motor. However, in contradiction to experimentally observed characteristic (c), the rotation starts at the edges. No report exists on employing the model for describing the AC motor. Theoreticians also attempted to explain the phenomena of the liquid film motor by focusing on the action of the mechanical moments on the liquid (Grosu and Bologna 2010). This enabled them to study the stationary rotation characteristics of the DC motor and to clarify its characteristics (b) and (c), but left characteristic (a) and the phenomena pertaining to the AC motor unexplained. In two very recent papers, we presented a model explicitly based on the intrinsic polarity of the liquids, which successfully explains all the observed characteristics of the DC and AC motors (Liu et al. 2011, 2012b).

The goal of our current article is to derive the dynamics of suspended polar liquid films, in particular water, when two crossed square-wave (SW) electric fields, i.e., a SW \mathbf{E}_{ext} and a SW \mathbf{E}_{el} with exactly the same frequencies are employed to induce EHD flows. This study is inspired by our recent finding that application of a DC \mathbf{E}_{ext} and a SW \mathbf{E}_{el} to water films leads to EHD motions differing from those of the DC or AC liquid film motors (Liu et al. 2012a). To the best of our knowledge, neither experimental nor theoretical investigations of EHD motions in water and other polar liquid films driven by \mathbf{E}_{ext} and \mathbf{E}_{el} , both with SW functional forms, have been undertaken. We will show that these SW fields, just as the DC and AC fields, may induce ordinary rotation. However, our analyses show that these SW fields have the advantageous additional property of inducing various reciprocating rotations. In the rest of this paper, we will refer to a polar liquid film driven by SW fields as a “SW liquid film device”.

As to the importance of our study, we foremost note that EHD rotations are commonly employed for mixing and

separations in microsystems. As such, our study has important implications for technological valuable apparatus such as micro-motors, micro-centrifuge, micro-mixers or drug delivery devices. Moreover, manipulations of flows in suspended polar liquid films illuminate their structural aspects. Detailed knowledge on the structure of such films is significant for research on the organization of liquid molecules in thin films, near container walls or biological membranes, e.g., the exclusion zone water phenomena currently intensively studied by the group of Prof. G.H. Pollack (Zheng et al. 2006). The importance of the characteristics of EHD motions studied in this paper compared with the findings of our previous publications on DC and AC polar liquid film motors is that it opens options for enhanced control of flow patterns.

The paper is organized as follows: in Sect. 2, we expand our model of the DC and AC motors to account for the specific EHD motions induced by the SW \mathbf{E}_{ext} and \mathbf{E}_{el} in the SW liquid film device. Specifically, we derive the general equations describing these motions. Their dynamical characteristics are investigated in Sect. 3. Summary and conclusions are presented in Sect. 4.

2 Model of water and polar liquid films

2.1 Suspended water and polar liquid films with applied \mathbf{E}_{ext} and \mathbf{E}_{el}

In our previous papers, we presented theoretical and experimental evidence for the assumption that a very thin water film or other polar liquid film in an \mathbf{E}_{ext} can be adequately modeled by a Bingham plastic fluid with an equivalent electric dipole moment (Liu et al. 2011, 2012b). Since the model is rather novel and lately additional supporting experimental evidence has accumulated, we concisely summarize these.

Quantum field theory (QFT) produces a picture of liquids composed of molecules with a sufficiently strong electric dipole moment (in the remainder of this paper referred to with the general term polar liquid, e.g., water or alcohol), as a mixture of two phases (Del Giudice et al. 1988):

1. A coherent phase made up of coherent domains (CDs). Quantum electro-dynamic (QED) interactions cause formation of the CDs. Within a CD, the polar liquid molecules coherently transit between two rotational states, oscillating in phase with a coherently condensed electromagnetic field.
2. A non-coherent phase made up of independent moving molecules, which are trapped in the interstices among the CDs. The rotational oscillations of these molecules are random.

During the past two decades, a series of theoretical and experimental studies, undertaken by several independent

research groups, evidenced the properties of the two phases of polar liquids and their roles in various phenomena (Del Giudice et al. 1988; Sivasubramanian et al. 2001a, b, 2002, 2003, 2005; Del Giudice and Vitiello 2006; Preparata 1995, 1988; Del Giudice and Preparata 1998; Del Giudice 2007; Emary and Brandes 2003; Apostol 2009; Yinnon and Yinnon 2009; Huang et al. 2009).

The CDs have an electric dipole moment. The CD's diameter typically reaches hundreds of micro-meters (μm) (Del Giudice et al. 1988, 2010a, b; Sivasubramanian et al. 2005; Del Giudice and Vitiello 2006). In bulk liquid these domains are oriented randomly, i.e., no net polarization exists. However, at interfaces, these domains are stabilized by the boundaries, resulting in a net polarization (Zheng et al. 2006; Sivasubramanian et al. 2005; Del Giudice and Vitiello 2006; Del Giudice et al. 1988, 2010a, b). External electric fields induce these CDs to organize in elongated super-domains, i.e., long ordered chains of low-entropy aligned coherent dipolar domains (Del Giudice et al. 2010a; Widom et al. 2009). (In the remainder of this paper, these chains will be denoted “super-CD”.) Such chain formation of dipolar spheres has also been identified by other approaches, e.g., integral equation theory in the reference hypernetted chain approximation, Monte Carlo and molecular dynamics simulations (Luo et al. 2011; Luo and Chen 2011). Two-dimensional neutron scattering has evidenced formation of such chain-like long-range molecular ordering within a D_2O bridge (Fuchs et al. 2010).

It is well known that polar particle chains are responsible for the unique characteristic of electrorheological fluids: with the application of an electric field, a Newtonian fluid instantaneously becomes a Bingham plastic fluid (Gandhi and Thompson 1992). In regard to the aforementioned, polar liquid films in an external electric field may be modeled as a Bingham plastic fluid with an equivalent dipole moment.

For a Bingham plastic fluid, for a simple shearing flow $u = u(y)$, the constitutive relation is (Bingham 1916; Steffe 1996):

$$\frac{\partial u}{\partial y} = \begin{cases} 0, & (\tau < \tau_0) \\ (\tau - \tau_0)/\mu, & (\tau \geq \tau_0) \end{cases} \quad (1)$$

where τ denotes the shear stress, τ_0 is the so-called yield stress, μ represents the plastic viscosity and y is the direction perpendicular to the flow velocity. Equation (1) indicates that flows occur in the liquid film, i.e., the film behaves like a fluid, when the shear stress is larger than the yield stress τ_0 .

For a polar liquid film located in an E_{ext} application of an electrolysis electric field E_{el} causing an electric current induces a torque (Liu et al. 2011). A sufficiently large E_{el} , crossing E_{ext} , will impede on the polarization equilibrium. However, E_{el} only exists within the liquid film. In contrast

E_{ext} , which plays a dominant role in the polarization, spans the whole space between two plates of a large parallel-plate capacitor. The strong correlated motions of the molecules in the super-CDs imply that it is impossible to touch one molecule without affecting all others (Preparata 1995, 1988; Del Giudice and Preparata 1998; Del Giudice 2007; Del Giudice et al. 2010b). Therefore E_{ext} will rapidly reestablish the polarization equilibrium. The continuous destructive effect of E_{el} on the polarization equilibrium maintained by E_{ext} creates a torque. (In the remainder of this paper, we refer to this torque as the “accelerating torque”.) In other words, the continuous competition between the destruction and the reestablishment of the polarization equilibrium may induce EHD motions in the liquid film.

The onset of rotation requires that the accelerating torque exerted on super-CDs is larger than the maximum static resistance torque arising from the yield stress. The magnitude of the accelerating torque depends on the direction and magnitude of the equivalent dipole moment per unit volume. In very thin films, the CDs are stabilized by the boundaries and the directions of the torques are perpendicular to the liquid film. However, in thick films or bulk liquids, the earlier mentioned absence of stabilization of the CD dipoles results in randomly oriented torques with magnitudes which decrease with the thickness of the film. Therefore, the onset of rotational motion depends on the thickness of the film. Indeed, experiments have shown that production of both DC and AC water motors requires films with a thickness of $<1 \mu\text{m}$ (Amjadi et al. 2009; Shirsavar et al. 2011).

Since only in sufficiently thin films crossed electric fields can induce rotations or vibrations, the polar liquid film can be modeled as a flat (two-dimensional) liquid, i.e., it may be assumed that its height h equals 0 (Liu et al. 2011, 2012b).

Based on the experimentally observed stable disk-like rings structure of the rotating liquid films, i.e., two-dimensional disks with radius r and width dr , the film may be modeled as a series of concentric circular disks in a polar coordinate system (r, θ) (Liu et al. 2011, 2012b).

2.2 EHD motions in water and polar liquid films

By applying the rotational form of Newton's second law to a single disk of water or other polar liquid films, in Liu et al. (2011, 2012b), we derived their dynamical equation in crossed E_{ext} and E_{el} , i.e.,

$$u_t = \frac{\mu}{\rho r^2} (r^2 u_{rr} + r u_r - u) + \frac{\Delta(t)}{\rho r}, \quad (0 \leq r \leq R, \quad t > 0). \quad (2)$$

Here u_t denotes the first partial derivative of the linear velocity $u(r, t)$ of the disk's rotation with respect to

time t ; u_r and u_{rr} , respectively, represent the first and the second partial derivative of $u(r, t)$ with respect to radius r ; ρ is the density of the fluid; $\Delta(t)$ is the driving source of the motions of the liquid film at time t , i.e., it represents the resultant moment exerted on the liquid film.

To expound the functional form of $\Delta(t)$, derived in Liu et al. (2011), we let M_{am} and M_f , respectively, symbolize the maximum of the accelerating torque and the maximum static resistance (drag) torque. When $M_{am} < M_f$, $\Delta(t) = 0$, i.e., the film remains static. When $M_{am} > M_f$, $\Delta(t) \neq 0$ and EHD motions appear in the film. The instantaneous value of $\Delta(t)$ is $|B(t)| - 2\tau_0$, where $B(t)$ and $-2\tau_0$, respectively, represent the accelerating torque and the drag torque exerted on the liquid film. The expression for $B(t)$ was derived in Sec. IV of Liu et al. (2011): $B(t) = \varepsilon_0(1 - 1/\varepsilon_r)E_{ext}(t)E_{el}(t)\sin\theta_{EJ}$, where ε_0 and ε_r , respectively, are the dielectric constant of the vacuum and the relative dielectric constant of the liquid; $E_{ext}(t)$ and $E_{el}(t)$, respectively, denote the magnitudes of \mathbf{E}_{ext} and \mathbf{E}_{el} at time t . θ_{EJ} is the angle between \mathbf{E}_{ext} and \mathbf{E}_{el} (or \mathbf{J}_{el}). In the current paper, we set $\theta_{EJ} = \pi/2$. Since the resultant torque is perpendicular to the liquid film, pointing ‘up’ or ‘down’, $\Delta(t)$ may be described by $|B(t)| - 2\tau_0$ or $-[|B(t)| - 2\tau_0]$. Thus, $\Delta(t)$ reads:

$$\Delta(t) = \begin{cases} 0, & (|B(t)| < 2\tau_0) \\ B(t) - 2\tau_0, & (B(t) \geq 2\tau_0) \\ B(t) + 2\tau_0, & (B(t) \leq -2\tau_0) \end{cases} \quad (3)$$

The second and third equations in Eq. (3) indicate that on defining $|B(t)|_{\max}$ as the maximum of $|B(t)|$, the inequality $|B(t)|_{\max} \geq 2\tau_0$ is a criterion for generation of EHD flows in the liquid film, that is, the equation

$$|B(t)|_{\max} = 2\tau_0 \quad (4)$$

determines the threshold fields required to start the film’s EHD flows.

To describe the EHD flow of the liquid film, Eq. (2) must obey two boundary conditions and an initial condition: the disappearance of the linear velocity at $r = 0$ and $r = R$ (where $R = l/2$ is half of the side-length l of a square film or the radius of a circle shaped film), and the liquid film is at rest at $t = 0$, i.e.,

$$u(r, t)|_{r=0} = 0, \quad u(r, t)|_{r=R} = 0 \quad (5)$$

and

$$u(r, t)|_{t=0} = 0. \quad (6)$$

Equation (2) is a typical diffusion equation with source. The general solution to it can be deduced by Green function technique (Courant and Hilbert 1989). It reads

$$u(r, t) = \int_0^t d\varsigma \int_0^R G(r, t; \xi, \varsigma) f(\xi, \varsigma) d\xi, \quad (7)$$

where

$$G(r, t; \xi, \varsigma) = \sum_{n=1}^{\infty} \frac{2\xi}{R^2 J_0^2(\kappa_n)} J_1\left(\frac{\kappa_n r}{R}\right) \times J_1\left(\frac{\kappa_n \xi}{R}\right) e^{-\frac{\mu \kappa_n^2}{\rho R^2}(t-\varsigma)}, \quad (8)$$

$$f(\xi, \varsigma) = \frac{\Delta(\varsigma)}{\rho \xi}. \quad (9)$$

Here κ_n denotes the n th zero point of $J_1(Z)$ ordinary Bessel function of order one, and $J_0(Z)$ is ordinary Bessel function of order zero.

3 Dynamics of SW liquid film devices

We assume $\mathbf{E}_{ext}(t)$ and $\mathbf{E}_{el}(t)$ have the following SW field forms, which are plotted in Fig. 1a:

$$E_{ext}(t) = \begin{cases} E_{ext}, & (0 \leq t < T/2) \\ -E_{ext}, & (T/2 \leq t < T) \end{cases}, \quad (10)$$

and

$$E_{el}(t) = \begin{cases} -E_{el}, & (0 \leq t < t_1 \text{ or } T/2 + t_1 \leq t < T) \\ E_{el}, & (t_1 \leq t < T/2 + t_1) \end{cases}, \quad (11)$$

where T denote the periods of $E_{ext}(t)$ and $E_{el}(t)$, t_1 is associated with the phase difference $\Delta\varphi$ between the fields $\mathbf{E}_{ext}(t)$ and $\mathbf{E}_{el}(t)$, i.e., $\Delta\varphi = 2\pi t_1/T$.

By inserting Eqs. (10) and (11) into the second and third equations in Eq. (3), we obtain the driving source $\Delta(t)$ as a function of t , which we plot in Fig. 1b. This figure shows that $\Delta(t)$ is a function with a period $T_d = T/2$ and

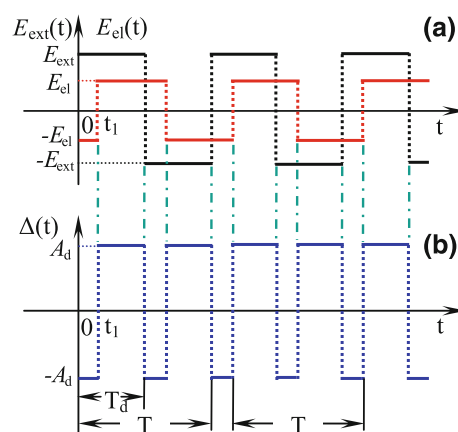


Fig. 1 **a** Sketch of the crossed SW $E_{ext}(t)$ and $E_{el}(t)$ versus time t ; **b** sketch of the driving source $\Delta(t)$ versus time t . T denote the periods of $E_{ext}(t)$ and $E_{el}(t)$, and T_d denotes the period of $\Delta(t)$

$$\Delta(t) = \begin{cases} -A_d, & (0 \leq t < t_1) \\ A_d, & (t_1 \leq t < T_d) \end{cases}, \quad (12)$$

where $A_d = \varepsilon_0(1 - 1/\varepsilon_r)E_{\text{ext}}E_{\text{el}}\sin\theta_{EJ} - 2\tau_0$. A change in the sign of $E_{\text{ext}}(t)$ or $E_{\text{el}}(t)$ corresponds to a reversal of the direction of these fields. Similarly, a change in the sign of $\Delta(t)$ corresponds to a reversal of the direction of the resultant torque exerted on the film. Equation (12) and Fig. 1b show that except for two special cases $t_1 = 0$ and $t_1 = T_d/2$, the driving source $\Delta(t)$ has a rectangular-wave form with period T_d . For $t_1 = 0$, the driving source $\Delta(t)$ does not change with time; it is constant. For $t_1 = T_d/2$, the driving source $\Delta(t)$ has a SW form with period T_d .

Recalling the aforementioned criterion Eq. (4) and letting $A_d = 0$, we obtain that the threshold fields to generate EHD flows in the SW liquid film device obey the following scaling relation:

$$E_{\text{ext}}U_{\text{el}}\sin\theta_{EJ} = \pm \frac{2\tau_0 l}{\varepsilon_0(1 - 1/\varepsilon_r)}. \quad (13)$$

Here $U_{\text{el}} = E_{\text{el}}l$ is used; $l = 2R$ denotes the side-length of the electrolysis cell. Equation (13) is the same as the scaling relation of the threshold fields for the DC motor (Liu et al. 2011). This indeed is to be expected, because the magnitudes of the accelerating torques for both the SW liquid film device and the DC motor are constant.

Since $\Delta(t)$ is a periodic function, on defining its period as $T_d = 2\pi/\omega$, its Fourier series expansion is

$$\Delta(t) = \sum_{m=0}^{\infty} (D_m \cos m\omega t + H_m \sin m\omega t), \quad (14)$$

where coefficients D_m and H_m are

$$\begin{aligned} D_0 &= A_d(1 - 2t_1/T_d), \quad D_m = -(2A_d \sin m\omega t_1)/m\pi, \\ H_m &= 2A_d(\cos m\omega t_1 - 1)/m\pi, \quad m = 1, 2, 3, \dots \end{aligned} \quad (15)$$

Using Eqs. (7)–(9), (14) and (15), we have (Liu et al. 2012a, b)

$$u(r, t) = \sum_{m=0}^{\infty} \sum_{n=1}^{\infty} C_n D_m J_1\left(\frac{\kappa_n r}{R}\right) F_{m,n}(t). \quad (16)$$

where

$$\begin{aligned} F_{m,n}(t) &= \frac{\cos \gamma_{m,n}}{\cos \phi_m} [\cos(m\omega t - \phi_m - \gamma_{m,n}) \\ &\quad - e^{-a_n t} \cos(\phi_m + \gamma_{m,n})], \end{aligned} \quad (17)$$

and

$$C_n = \frac{2R(1 - J_0(\kappa_n))}{\mu \kappa_n^3 J_0^2(\kappa_n)}, \quad a_n = \frac{\mu \kappa_n^2}{\rho R^2}, \quad (18)$$

$$\phi_m = \arctan(H_m/D_m), \quad \gamma_{m,n} = \arctan(m\omega/a_n). \quad (19)$$

The related angular velocity is

$$\omega(r, t) = u(r, t)/r. \quad (20)$$

Equations (16) and (20) show that the rotation angular velocity consists of a lot of spatial modes expressed by a series of functions $J_1(\kappa_n \chi)/\chi$, $\chi \in [0, 1]$, $n = 1, 2, \dots$. Since $J_1(\kappa_n \chi)/\chi$ is a decreasing function of variable χ , from the mathematical viewpoint one can easily understand that the particles close to the film's center are rotating faster than those far away from it.

3.1 Effects of the phase difference on dynamics of SW liquid film devices

3.1.1 Effects of the phase difference on dynamics for $t_1 = 0$

For $t_1 = 0$ (or $t_1 = T_d$), i.e., $\Delta\varphi = 0$ (or $\Delta\varphi = \pi$), from Eq. (15) we have $D_0 = A_d$ (or $D_0 = -A_d$), $D_m = H_m = 0$, $m = 1, 2, 3, \dots$. Inserting these coefficients into Eq. (16), we obtain the film's rotation linear velocity driven by the in-phase (or anti-phase) SW fields:

$$u(r, t) = D_0 \sum_{n=1}^{\infty} C_n J_1\left(\frac{\kappa_n r}{R}\right) (1 - e^{-a_n t}), \quad (21)$$

where C_n and a_n are given by Eq. (18). Equation (21) shows that for $\Delta\varphi = 0$ (or π), the dynamical characteristics of the SW liquid film device are the same as those of the DC motor, which is detailed in Sec. IV of Liu et al. (2011), i.e., for $t_1 = 0$ (or $t_1 = T_d$) the SW liquid film device exhibits a simple anticlockwise (or clockwise) rotation. It constitutes a centrifuge or motor.

3.1.2 Effects of the phase difference on dynamics for $t_1 = T_d/2$

For $t_1 = T_d/2$, i.e., $\Delta\varphi = \pi/2$, from Eq. (15) we obtain $D_0 = D_m = 0$, $H_m = 2A_d[(-1)^m - 1]/m\pi$ ($m = 1, 2, 3, \dots$). Thus, Eq. (16) becomes

$$\begin{aligned} u(r, t) &= \sum_{m=1}^{\infty} \sum_{n=1}^{\infty} C_n H_m J_1\left(\frac{\kappa_n r}{R}\right) \cos \gamma_{m,n} \\ &\quad \times [\sin(m\omega t - \gamma_{m,n}) + e^{-a_n t} \sin \gamma_{m,n}]. \end{aligned} \quad (22)$$

To illuminate the dynamical characteristics of the SW liquid film devices for this $t_1 = T_d/2$ value, we adopt the experimental parameters of the exemplary extensively measured and theoretically investigated DC water film motor, i.e.: $\varepsilon_0 = 8.85 \times 10^{-12} \text{ F m}^{-1}$, $\varepsilon_r = 80$, $E_{\text{ext}}U_{\text{el}}\sin\theta_{EJ} = 1.44 \times 10^7 \text{ V}^2 \text{ m}^{-1}$, $l = 2R = 1.2 \times 10^{-2} \text{ m}$, $\mu = 10^{-3} \text{ Pa s}$ and its derived $\tau_0 = 6.77 \times 10^{-5} \text{ Pa}$ (Shirsavar et al. 2006, 2011; Amjadi et al. 2008, 2009;

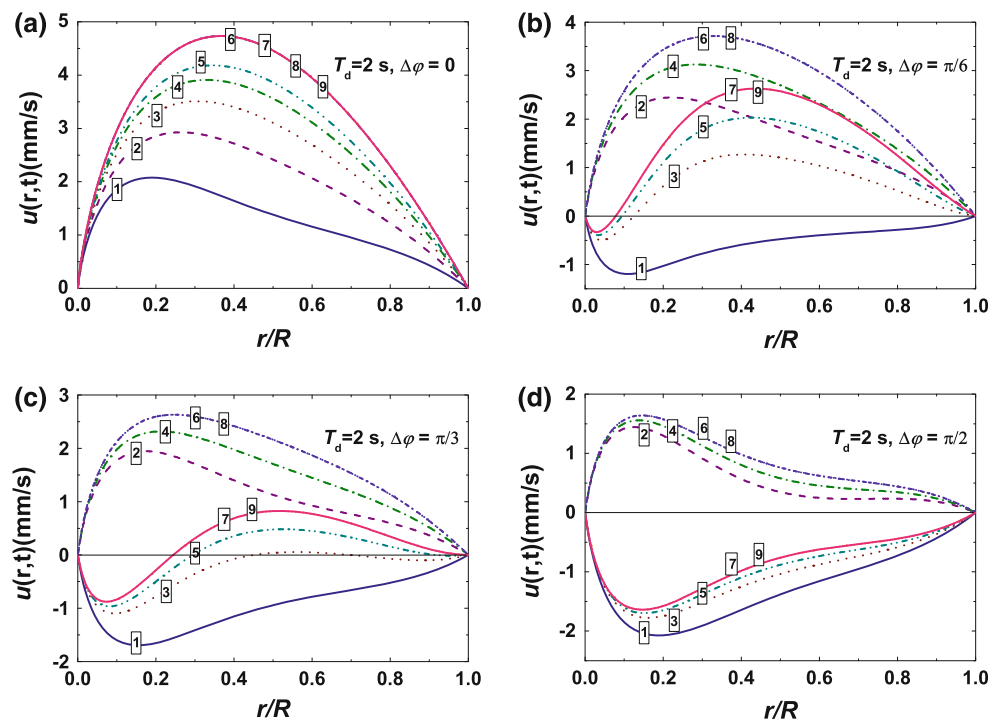
Liu et al. 2011). Employing Eqs. (21), (22) and these parameters, we, respectively, plotted the cross-radial (tangential) velocity profiles for two cases $\Delta\varphi = 0$ and $\Delta\varphi = \pi/2$ when $T_d = 2$ s (see Fig. 2a, d). Labels 1–9 on the curves in Fig. 2, respectively, denote nine times: $t_1, T_d, T_d + t_1, n_1 T_d, n_1 T_d + t_1, n_2 T_d, n_2 T_d + t_1, n_3 T_d, n_3 T_d + t_1$. In Fig. 2a and d, $t_1 = 1$ s and $n_1 = 2, n_2 = 10, n_3 = 100$. Figure 1b illustrates that the driving source changes sign at these chosen times, i.e., the net torque exerted on the liquid film changes direction at these time. Thus, the film's rotation speed reaches its maxima or minima at these times, i.e., the curves in Fig. 2 draw the outline of the rotating liquid film at time t .

Figure 2a indicates that for $\Delta\varphi = 0$, for small t values, the film's anticlockwise rotation speed increases and after about 20 s it stabilizes. In contrast, Fig. 2d shows that for $\Delta\varphi = \pi/2$ the liquid film exhibits a periodic reversal. In the first half of a period from $t = 0$ to $t = T_d/2$, the liquid film rotates clockwise. At $t = T_d/2$ the rotation speed of the liquid film is a minimum (see curve 1 in Fig. 2d), because the net torque exerted on the liquid film changes sign when the direction of the electric field reverses. In the next half of a period the film will rotate anticlockwise and its speed reaches a maximum at $t = T_d$, see curve 2 in Fig. 2d. In the interval from $t = T_d$ to $t = 3T_d/2$, the film rotates clockwise once again. The repetitive changes in the direction of the rotations and the vanishing of the transient process characterized by terms with $e^{-a_n t}$ in Eq. (22), for sufficiently large t , lead the film to exhibit a symmetrical

reciprocating rotation. In other words, for these conditions, the SW liquid film device constitutes a washing machine. As derived in Liu et al. (2012a), similar symmetrical reciprocating rotations can be produced by applying DC E_{ext} and SW E_{el} fields to polar liquid films.

Some features, for which future direct experimental verification will provide additional support for our model, hide behind the above derived symmetrical reciprocating rotation of the liquid film. The features also appears when E_{ext} and E_{el} , respectively, have a DC and SW shape (Liu et al. 2012a). To elucidate it, in Fig. 3 we plot for a film in applied SW E_{el} and SW E_{ext} the tangential velocity profiles versus radius for six times in a half a period from $t = 20.0$ s to $t = 21.0$ s. A similar plot for a film in an applied SW E_{el} and DC E_{ext} is presented in Fig. 3 of Liu et al. (2012a). Curves labeled 6 and 7 in Fig. 3 (of our current paper) are the same as those with the same labels in Fig. 2d. Figure 3 shows that particles near the center of the liquid film reverse their direction earlier (see curve a) than those farther away from the center (see curve b). Ultimately, the whole liquid film rotates clockwise (see curves c, d and 7). These theoretically derived rotational characteristics are the same as those experimentally observed for the DC motors. Experimentalists have observed the reversal characteristics of the DC motor by intermittently changing the direction of E_{el} while keeping E_{ext} constant. According to the experimental videos available on <http://www.softmatter.cscm.ir/FilmMotor/>, immediately after application of electric fields, the rotating spiral curves emerging near the center of the

Fig. 2 Tangential velocity profiles versus radius r (in units of R) for nine times t , defined in the text and symbolized with numbers within rectangles. **a–d** Several phase difference: for $\Delta\varphi = 0$, the liquid rotates anticlockwise; for $\Delta\varphi = \pi/2$, it exhibits a symmetrical reciprocating rotation; for $0 < \Delta\varphi < \pi/2$, it presents an asymmetrical reciprocating rotation



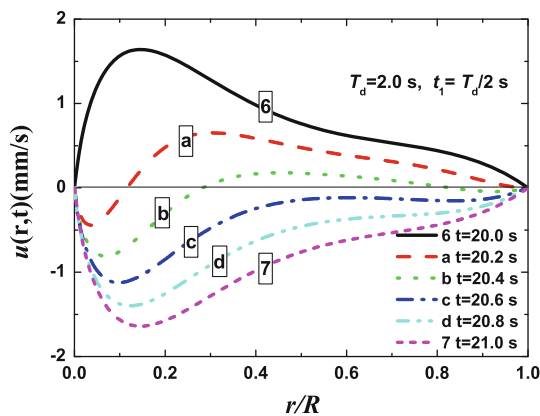


Fig. 3 Tangential velocity profiles versus radius r (in units of R) for six times in an interval from $t = 20.0$ s to $t = 21.0$ s

films indicate that the region near the center of the film rotates faster than the more outward lying regions. Video 8 shows that on the passage of time, the spiral-like rotation curves first spread all over the film and subsequently disappear. In the steady state only circled rotation curves cover the film. Video 2 shows that immediately after the reversal of the electrolysis field E_{el} , the color change of the central area of the film is significantly faster than that of the surrounding area. The correspondence between these rotational characteristics of the SW liquid film devices and the experimental DC motor support our theoretical predictions. However, further detailed experiments, involving applied SW fields to polar liquid films, are required for ultimate verification of these predictions.

3.1.3 Effects of the phase difference on dynamics for $0 < t_1 < T_d/2$

For $0 < t_1 < T_d/2$, i.e., $0 < \Delta\phi < \pi/2$, on employing Eqs. (15) and (16) and the same parameters as in Fig. 2a and d, we plot in Fig. 2b and c the tangential velocity profiles versus radius, respectively, for $\Delta\phi = \pi/6$ and $\Delta\phi = \pi/3$ at the nine typical times mentioned above with $t_1 = 1/3$ s in Fig. 2b and $t_1 = 2/3$ s in Fig. 2c. Figure 2b and c show that after lots of repetitive reversals, the liquid film ultimately exhibits an asymmetrical reciprocating rotation. In other words, the SW liquid film device constitutes a mixer. Curves 7 and 9 in Fig. 2b and c predict that the region near the center of the film and that near the border may rotate in opposite directions. Figure 2b–d show that the reversal area close to the center increases with $\Delta\phi$ and for $\Delta\phi = \pi/2$, the reversal region extends all over the film.

Asymmetrical reciprocating rotations have not yet been identified for any of the polar liquid film devices studied in previous publications, i.e., the DC and AC liquid film

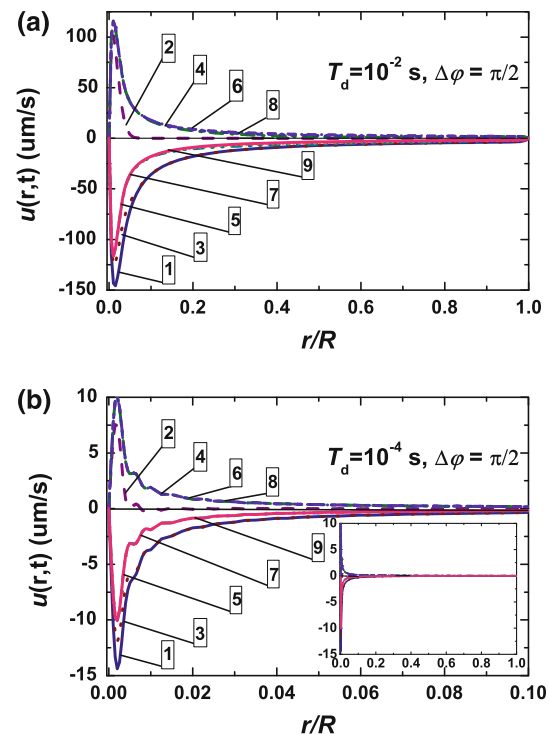


Fig. 4 Tangential velocity profiles versus radius r (in units of R) at nine times (defined in the text) when the film is driven by SW fields with phase difference $\Delta\phi = \pi/2$ and frequencies: **a** $f = f_d/2 = 50$ Hz; **b** $f = f_d/2 = 5$ kHz. The inset in **b** exhibits the outline of the tangential velocity profiles of the whole liquid film, i.e., $0 \leq r/R \leq 1$

motors or films in applied DC E_{ext} and SW E_{el} . Accordingly, the current section findings indicate that devices composed of polar liquid films with applied SW E_{ext} and SW E_{el} have a technologically advantageous property, which is not yet known to exist in other devices.

The results derived in Sects. 3.1.1–3.1.3 can be summarized as follows: when the frequency f_d of the driving source is small (e.g., $T_d = 1/f_d = 2$ s, as chosen above), the liquid film exhibits three rotational patterns for different $\Delta\phi$: an ordinary clockwise rotation ($\Delta\phi = 0$) or an ordinary anticlockwise rotation ($\Delta\phi = \pi$), a symmetrical reciprocating rotation ($\Delta\phi = \pi/2$) and an asymmetrical reciprocating rotation ($0 < \Delta\phi < \pi/2$). These rotations, respectively, enable the polar liquid (water) film driven by the SW fields to be a centrifuge, the smallest washing machine or a liquid film mixer.

3.2 Effects of the fields' frequencies on dynamics of SW liquid film devices

For $\Delta\phi = 0$, from Eq. (21) we see that the dynamical characteristics are independent of the field's frequency $f = 1/T$.

3.2.1 Effects of the fields' frequencies on dynamics for $\Delta\varphi = \pi/2$

For $\Delta\varphi = \pi/2$, in Fig. 4a and b, respectively, we plot tangential velocity profiles of the liquid film device driven by SW E_{ext} and SW E_{el} leading to driving sources with frequencies $f_d = 10^2$ Hz ($T_d = 1 \times 10^{-2}$ s) and $f_d = 10^4$ Hz ($T_d = 1 \times 10^{-4}$ s). Labels 1–9 on the curves in Fig. 4, respectively, denote nine typical times: $t_1, T_d, T_d + t_1, n_1 T_d, n_1 T_d + t_1, n_2 T_d, n_2 T_d + t_1, n_3 T_d, n_3 T_d + t_1$, where $t_1 = T_d/2, n_1 = 2f_d, n_2 = 4f_d, n_3 = 20f_d$. Other parameters used in plotting Fig. 4 are the same as those used to compute Fig. 2. Comparing Figs. 2d with 4, one finds that as f_d increases the liquid film exhibits similar dynamical characteristics to those shown in Fig. 2d. However, with increasing f_d : the rotation speed decreases rapidly (from mm/s to $\mu\text{m/s}$); only particles near the center of the film can reverse their rotational direction with the change of the sign of the applied electric fields; particles in outward laying regions almost do not move (see Fig. 4b and its inset). Similar features were observed for polar liquid films with applied DC E_{ext} and SW E_{el} (Liu et al. 2012a). Concerning these effects of increments in f_d , it is worth citing a result experimentally observed and theoretically derived, respectively, in Amjadi et al. (2009) and Liu et al. (2012b). The AC motor only vibrates in crossed cosine AC fields with different frequencies. From the above analysis, we infer that the origin and nature of the vibration of the liquid film is the high-frequency symmetric reciprocating rotation of the center region of the liquid film. This conjecture remains to be verified by further experiments.

3.2.2 Effects of the fields' frequencies on dynamics for $0 < \Delta\varphi < \pi/2$

For $0 < \Delta\varphi < \pi/2$ and relatively high f_d ($f \geq 50$ Hz), our computations show that the EHD flows do not vary strongly with f_d . Taking $f = f_d/2 = 50$ Hz as an example, we, respectively, plot the tangential velocity profiles in Fig. 5 for two cases: $\Delta\varphi = \pi/6$ ($t_1 = T_d/6$) and $\Delta\varphi = \pi/3$ ($t_1 = T_d/3$). Labels 1–9 on the curves in Fig. 5, respectively, denote nine typical times: $t_1, T_d, T_d + t_1, n_1 T_d, n_1 T_d + t_1, n_2 T_d, n_2 T_d + t_1, n_3 T_d, n_3 T_d + t_1$, where $n_1 = 2f_d, n_2 = 4f_d, n_3 = 20f_d$. By comparing Figs. 2b and c with 5, one discerns that (1) as f_d increases, at first the film exhibits an asymmetrical rotation (see the insets in Fig. 5), but ultimately the whole liquid film exhibits a simple anticlockwise rotation and that (2) the stable rotation speed diminishes with increasing phase difference $\Delta\varphi$, as can be learned from the maxima of curves 8 and 9 for $\Delta\varphi = \pi/6$ which are greater than those of the corresponding curves for $\Delta\varphi = \pi/3$. To expose the causes underlying these

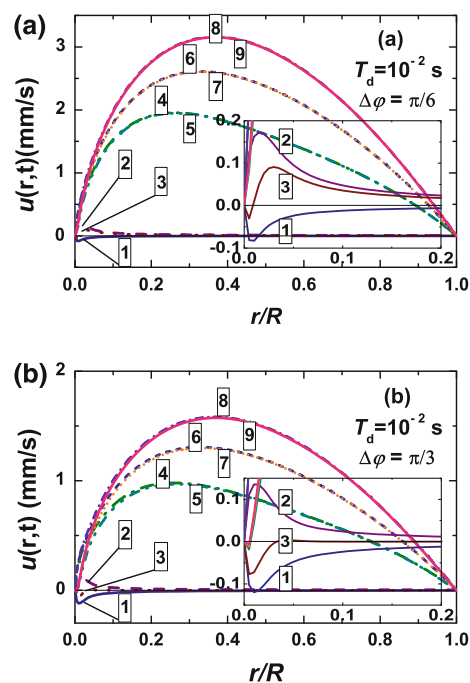


Fig. 5 Tangential velocity profiles versus radius r (in units of R) at nine typical times (defined in the text) for two different phase difference. **a** $\Delta\varphi = \pi/6$; **b** $\Delta\varphi = \pi/3$. In both cases, the frequencies of the SW electric fields are $f = f_d/2 = 50$ Hz. The insets are the enlarged graphs which illustrate curves 1, 2 and 3

findings, we analyze the relation between the driving source $\Delta(t)$ and the mean value of the stable rotation velocity $u(r, t)$ of the liquid film. Since the transient state process vanishes for sufficient long time, we only consider $u(r, t)$ without the transient-state terms, i.e., Eq. (16) becomes

$$u(r, t) = \frac{D_0}{2\mu} r \ln \frac{R}{r} + \sum_{m=1}^{\infty} \sum_{n=1}^{\infty} C_n D_m J_1 \left(\frac{\kappa_n r}{R} \right) \times \frac{\cos \gamma_{m,n}}{\cos \phi_m} \cos(m\omega t - \gamma_{m,n} - \phi_m). \quad (23)$$

From Eq. (23) we obtain the average linear velocity over a period T_d , i.e.,

$$\overline{u(r, t)} = \frac{\bar{\Delta}}{2\mu} r \ln \frac{R}{r}, \quad (24)$$

where $\bar{\Delta} = D_0 = A_d(1 - 2\Delta\varphi/\pi)$. Equation (24) helps us to understand the proportional relationship among the maxima of the curves 8 and 9 in Figs. 2a and 5. When $\Delta\varphi = 0, \pi/6$ or $\pi/3, \bar{\Delta}$, respectively, equals $A_d, 2A_d/3$ and $A_d/3$, and the associated maxima of the stable rotation speeds are, respectively, 4.8, 3.2 and 1.6 mm/s. When $\Delta\varphi = \pi/2, \bar{\Delta} = 0$ and $\overline{u(r, t)} = 0$. It is well known that the mean value of the velocity of a particle undergoing simple harmonic motion is zero. Accordingly, the symmetrical reciprocating rotation may be considered as a generalized

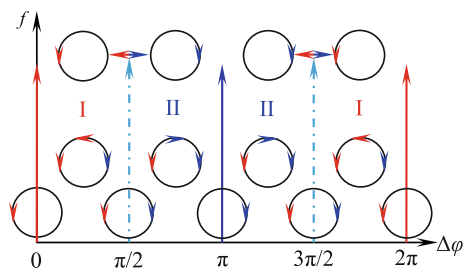


Fig. 6 The phase graph of the rotation modes of the SW liquid film device. The circles with one arrow denote a simple rotation (an anticlockwise rotation or a clockwise rotation) of the film. The circles with two or three arrows, respectively, denote a symmetric reciprocating or an asymmetric reciprocating rotation of the film. The short line with two opposite directed arrows represents the vibration of the liquid film. The three upward solid arrows exhibit that for $\Delta\varphi = 0, \pi$ and 2π , an ordinary anticlockwise or clockwise rotation is independent of f . The two dashed light blue arrows indicate that for $\Delta\varphi = \pi/2$ (or $3\pi/2$), a symmetric reciprocating rotation converts to a vibration as f increases. Region I shows that for $0 < \Delta\varphi < \pi/2$ and $3\pi/2 < \Delta\varphi < 2\pi$, an asymmetric rotation converts to an ordinary anticlockwise rotation when f increases. Region II shows that for $\pi/2 < \Delta\varphi < \pi$ and $\pi < \Delta\varphi < 3\pi/2$, an asymmetric rotation converts to an ordinary clockwise rotation when f increases (colour figure online)

two-dimensional simple harmonic motion of the liquid film. When f is sufficiently large, such a rotation exhibits itself as a vibration of the film.

Above we analyzed the dynamical characteristics of the SW liquid film device for $\Delta\varphi \subseteq [0, \pi/2]$. The associated study method and results can be generalized to $\Delta\varphi \subseteq [0, 2\pi]$. The main results are summarized in Fig. 6, which presents the phase graph of the rotation mode of the SW liquid film device.

4 Summary and conclusions

EHD rotations of suspended polar liquid (water) films, induced by applied SW electric fields, i.e., a SW E_{ext} and a SW E_{el} , are investigated by analytical derivation of their linear and angular velocity patterns. The investigation and in particular the phase graph of the rotational patterns, presented in Fig. 6, show that the films' EHD motions depend on the phase difference $\Delta\varphi$, the frequency f , and the magnitudes of the SW electric fields:

1. For $\Delta\varphi = 0$ (or π), simple anticlockwise (or clockwise) rotations may be induced, i.e., polar liquid films constitutes a centrifuge. Their speeds are independent of f .
2. For $\Delta\varphi = \pi/2$ (or $3\pi/2$), a symmetrical reciprocating rotation may be induced, i.e., the polar liquid film constitutes a washing machine. On increasing f above a liquid specific transition value, a change from rotation to vibration takes place.

3. For $\Delta\varphi$ with values differing from those mentioned in the previous paragraphs (1) and (2) and for f of about 0.1–1 Hz, an asymmetrical reciprocating rotation may be induced, with the region near the center of the film and the region near the border rotating in opposite directions, i.e., the polar liquid film constitutes a mixer. For f above a liquid specific value, typical ~ 1 Hz, a simple anticlockwise (see region I in Fig. 6) [or clockwise (see region II in Fig. 6)] rotation may be induced.

As to potential refinements of our liquid film model, we note that inclusion of mass transfer between the circular disks may be desirable for fine-tuning values of f and magnitudes of E_{ext} and E_{el} required to induce the various rotations. A future study, examining such mass transfer in reciprocating rotations might also illuminate the fluid nature of the film.

The main contributions of this paper's analyses of SW water and polar liquid film devices are

1. Identification of new types of EHD flows in water and polar liquid films, which have significant technological potential.
2. Identification of an additional technique for studying water and polar liquid films. With the dependence of the rotational modes of the SW polar liquid film device on the phase difference $\Delta\varphi$, the frequency f and the magnitudes of the SW electric fields, the device can be employed to extract information on the structure and dynamics of its liquid film.
3. Complementarity and reinforcement of our previous consistent successful explanations of characteristics of the AC water film motor, e.g., the finding in Sect. 3.2.1 that the origin and nature of the vibration of the AC motor's liquid film is the high-frequency symmetric reciprocating rotation of the center region of the liquid film.

The results derived in this paper have yet to be experimentally verified. Our model's recent successes, pertaining to explanation of the experimentally identified characteristics of the closely related polar liquid films with applied DC and AC electric fields, suggests verification of this paper's findings is a worthwhile project. Verification of our predictions will (a) provide additional tools for researching the structure and dynamics of polar liquid (water) films in applied electric fields, (b) will provide additional support for the assumption that a polar (water) film in an applied E_{ext} behaves as a Bingham plastic fluid and (c) widen the scope of research on water films with potential important technological applications, e.g., micro-washing machines, centrifuges, mixers.

Acknowledgments This work is supported by the National Basic Research Program of China (Grant No. 2007CB815105), National Natural Science Foundation of China (Grant Nos. 11074300, 10775088) and Shandong Natural Science Foundation under (Grant No. ZR2011AM018). Z.-Q. Liu and S.-R. Jiang gratefully thank Dr. Tamar A. Yinnon for her patient guidance, encouragement, enlightening discussions, warm support and proof reading of this manuscript.

References

- Amjadi A, Shirsavar R, Radja NH, Ejtehadi MR (2008) A liquid film motor. arXiv:0805.0490 [cond-mat.soft]
- Amjadi A, Shirsavar R, Radja NH, Ejtehadi MR (2009) A liquid film motor. *Microfluid Nanofluid* 6:711
- Apostol M (2009) Coherence domains in matter interacting with radiation. *Phys Lett A* 373:379
- Bingham EC (1916) An investigation of the laws of plastic flow. *Bull US Bur Stand* 13:309
- Courant R, Hilbert D (1989) *Methods of mathematical physics*. Wiley, New York
- Daya ZA, Morris SW, de Bruyn JR (1997) Electroconvection in a suspended fluid film: a linear stability analysis. *Phys Rev E* 55:2682
- Del Giudice E (2007) Old and new views on the structure of matter and the special case of living matter. *J Phys Conf Ser* 67:012006
- Del Giudice E, Preparata G (1998) *Macroscopic quantum coherence*. World Scientific, Singapore
- Del Giudice E, Vitiello G (2006) Role of the electromagnetic field in the formation of domains in the process of symmetry-breaking phase transitions. *Phys Rev A* 74:022105
- Del Giudice E, Preparata G, Vitiello G (1988) Water as a free electric dipole laser. *Phys Rev Lett* 61:1085
- Del Giudice E, Fuchs EC, Vitiello G (2010a) Collective molecular dynamics of a floating water bridge. *Water* 2:69
- Del Giudice E, Spinetti PR, Tedeschi A (2010b) Water dynamics at the root of metamorphosis in living organisms. *Water* 2:566
- El-Ali J, Sorger PK, Jensen KF (2006) Cells on chips. *Nature* 442:403
- Emary C, Brandes T (2003) Chaos and the quantum phase transition in the Dicke model. *Phys Rev E* 67:066203
- Faetti S, Fronzoni L, Rolla PA (1983a) Static and dynamic behavior of the vortex-electrohydrodynamic instability in freely suspended layers of nematic liquid crystals. *J Chem Phys* 79:5054
- Faetti S, Fronzoni L, Rolla PA (1983b) Electrohydrodynamic domain patterns in freely suspended layers of nematic liquid crystals with negative dielectric anisotropy. *J Chem Phys* 79:1427
- Fuchs EC, Baroni P, Bitschnau B, Noirez L (2010) Two-dimensional neutron scattering in a floating heavy water bridge. *J Phys D Appl Phys* 43:105502
- Gandhi MV, Thompson BS (1992) *Smart materials and structures*. Chapman & Hall, London
- Grosu FP, Bologa MK (2010) Electroconvective rotation of a dielectric liquid in external electric fields. *Surf Eng Appl Electrochem* 46:43
- Huang C, Wikfeldt KT, Tokushima T, Nordlund D, Harada Y, Bergmann U, Niebuhr M, Weiss TM, Horikawa Y, Leetmaa M, Ljungberg MP, Takahashi O, Lenz A, Ojamäe L, Lyubartsev AP, Shin S, Pettersson LGM, Nilsson A (2009) The inhomogeneous structure of water at ambient conditions. *Proc Natl Acad Sci USA* 106:15214
- Liu ZQ, Li YJ, Zhang GC, Jiang SR (2011) Dynamical mechanism of the liquid film motor. *Phys Rev E* 83:026303
- Liu ZQ, Gan KY, Li YJ, Zhang GC, Jiang SR (2012a) Electrohydrodynamical characteristics of liquid film motor driven by a square-wave electrophoresis electric field. *Acta Phys Sin* 61:134703
- Liu ZQ, Zhang GC, Li YJ, Jiang SR (2012b) Water film motor driven by alternating electric fields: its dynamical characteristics. *Phys Rev E* 85:036314
- Luo L, Chen XS (2011) Chain formation in a monolayer of dipolar hard spheres under an external field. *Sci China Phys Mech Astron* 54:1555
- Luo L, Klapp SHL, Chen XS (2011) String formation and demixing in monolayers of dipolar colloidal mixtures. *J Chem Phys* 135:134701
- Morris SW, de Bruyn JR, May AD (1990) Electroconvection and pattern formation in a suspended smectic film. *Phys Rev Lett* 65:2378
- Preparata G (1988) Quantum field theory of the free-electron laser. *Phys Rev A* 38:233
- Preparata G (1995) *QED coherence in matter*. World Scientific, Singapore
- Ramos A, Morgan H, Green NG, Castellanos A (1998) Ac electrokinetics: a review of forces in microelectrode structures. *J Phys D Appl Phys* 31:2338
- Shirsavar R, Amjadi A, Radja NH, Nirya MD, Tabar MRR, Ejtehadi MR (2006) A water film motor. arXiv:condmat/0605029 [cond-mat.soft]
- Shirsavar R, Amjadi A, Tonddast-Navaei A, Ejtehadi MR (2011) Electrically rotating suspended films of polar liquids. *Exp Fluids* 50:419
- Shiryaeva EV, Vladimirov VA, Zhukov MY (2009) Theory of rotating electrohydrodynamic flows in a liquid film. *Phys Rev E* 80:041603
- Sivasubramanian S, Widom A, Srivastava YN (2001a) Gauge invariant formulations of Dicke–Preparata super-radiant models. *Physica A* 301:241
- Sivasubramanian S, Widom A, Srivastava YN (2001b) Super-radiance and the unstable photon oscillator. *Int J Mod Phys B* 15:537
- Sivasubramanian S, Widom A, Srivastava YN (2002) Landau ghosts and anti-ghosts in condensed matter and high density hadronic matter. *Mod Phys Lett B* 16:1201
- Sivasubramanian S, Widom A, Srivastava YN (2003) Microscopic basis of thermal superradiance. *J Phys Condens Matter* 15:1109
- Sivasubramanian S, Widom A, Srivastava YN (2005) The Clausius–Mossotti phase transition in polar liquids. *Physica A* 345:356
- Sonin AA (1998) *Freely suspended liquid crystalline films*. Wiley, New York
- Squires TM, Quake SR (2005) Microfluidics: fluid physics at the nanoliter scale. *Rev Mod Phys* 77:977
- Steffe JF (1996) *Rheological methods in food process engineering*. Freeman Press, East Lansing
- Widom A, Swain J, Silverberg J, Sivasubramanian S, Srivastava YN (2009) Theory of the Maxwell pressure tensor and the tension in a water bridge. *Phys Rev E* 80:016301
- Yinnon CA, Yinnon TA (2009) Domains in aqueous solutions: theory and experimental evidence. *Mod Phys Lett B* 23:1959
- Zheng JM, Chin WC, Khijniak E, Khijniak E Jr, Pollack GH (2006) Surfaces and interfacial water: evidence that hydrophilic surfaces have long-range impact. *Adv Colloid Interface Sci* 127:19